Sei Ueda, et.al. International Journal of Engineering Research and Applications
www.ijera.com
ISSN: 2248-9622, Vol. 16, Issue 6, June 2026, pp 22-32

RESEARCH ARTICLE OPEN ACCESS

Temperature Rise Induced by a Joule Heating Effect of a Disturbed Current Density in a Plate with an Axisymmetric Crack During Resistance Spot Welding

Sei Ueda*, Daisuke Kugishima*, Ryouta Imada* and Yuuki Mori*
**(Department of Mechanical Engineering, Osaka Institute of Technology, Japan, Email: sei.ueda@oit.ac.jp)*

ABSTRACT
In this paper, we consider the temperature distribution in a plate with an axisymmetric crack (an annular crack and a penny-shaped crack) during resistance spot welding under a uniform current density. In the calculations, the crack faces are supposed to be electrically and thermally insulated. The Hankel integral transform method is applied to reduce the electric problem to a singular integral equation, which is solved numerically by using the Gauss-Chebyshev or Gauss-Jacobi integration formula. With the solution of the singular integral equation, we can get the disturbed electric field. Furthermore, by solving the Poisson's equation with a heat generation induced by the disturbed current density components, we can obtain the disturbed temperature distribution. Numerical calculations are carried out, and the detailed results presented to illustrate the influence of the geometric parameters on the electric and thermal fields.

Keywords **-** Resistance spot welding, Disturbed current density, Joule heating effect, Temperature rise, Hankel transform, Singular integral equation

---

Date of Submission: 06-06-2026 Date of acceptance: 16-06-2026

I. Introduction

The equipment used in the resistance spot welding process consists of tool holders and electrodes. The current from the electrodes is applied and the contacted metal surfaces are joined by the heat obtained from resistance to current density components, that is, the Joule heating effect. Then, if there are some defects in the metal, such as cracks, the current density components will be disturbed by the crack, and an unexpected temperature distribution will be induced and may cause some troubles in the welding process. However, except for Liu's study [1], very few investigations on these phenomena have been made. Therefore, we treated the disturbed electric and thermal problems of a plate with a through crack during resistance spot welding under a uniform current density [2], and we could also get the closed form solution for a special case. But, from a practical standpoint, the three-dimensional approach for this problem should be required.

In this study, the electric and thermal problems for a plate with an axisymmetric crack (an annular crack and a penny-shaped crack) during resistance spot welding under a uniform current density is considered. The crack surfaces are supposed to remain electrically and thermally insulated. The Hankel integral transform technique is used to reduce the electric problem to the solution of the singular integral equation [3]. Using the Gauss-Chebyshev or Gauss-Jacobi integration formula [4], the solution of the singular integral equation is obtained. The disturbed electric field can be calculated with the obtained solution. Furthermore, by solving the Poisson's equation with a heat generation induced by the disturbed current density components, we can get the disturbed temperature distribution. Some results are presented to illustrate the influence of the geometric parameters on the electric and temperature fields.

II. Formulation of the Problem

Consider an infinite long plate of thickness $h = h_1 + h_2$ with the cylindrical coordinate system (r, θ, z), as shown in Fig. 1. The plate has an annular crack which is supposed to occupy the region $0 \le a < r < b \quad (b - a = 2c)$, $z = 0$ in the plate, where $2c$ denotes the width of the crack. For the case of $a = 0$, the crack becomes a penny-shaped

crack of the radius $2c$. We assume that the current density components in the z -direction $J_{zi}(r,z)\,(i=1,2)$ at the top surface $(z=h_1)$ and the bottom surface $(z=-h_2)$ are maintained at $J_{z1}(r,h_1)=J_{z2}(r,-h_2)=-J_0 \quad (0\le r<\infty)$, where J_0 indicates the constant current density. The temperatures $T_i(r,z)\,(i=1,2)$, which are induced by the disturbed current density components, at the surfaces are fixed to $T_1(r,h_1)=T_2(r,-h_2)=0$ $(0\le r<\infty)$, respectively. The crack surfaces are supposed to remain electrically and thermally insulated. In the following, the subscript $i=1,2$ denotes the electric and thermal fields in $0\le z\le h_1$ and $-h_2\le z\le 0$, and the subscripts r,z will be used to refer to the direction of coordinates. The electric conductivity and the thermal conductivity are denoted by κ and λ.

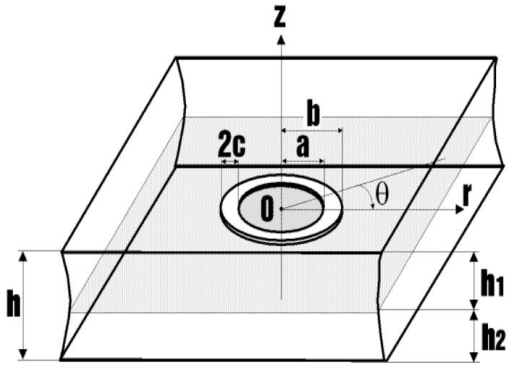

Fig. 1 An annular crack in a conducting plate

III. Electric Fields

The electric potentials $\Phi_i(r,z)\,(i=1,2)$ are given by the sums of the non-disturbed component $\Phi^{(1)}(z)$ and the disturbed components $\Phi_i^{(2)}(r,z)$ $(i=1,2)$ as follows:

$$\Phi_i(r,z)=\Phi^{(1)}(z)+\Phi_i^{(2)}(r,z) \quad (i=1,2) \tag{1}$$

It is easy to find that $\Phi^{(1)}(z)$ is:

$$\Phi^{(1)}(z)=\frac{J_0}{\kappa}\left(z+h_2\right) \tag{2}$$

The non-disturbed current density components $J_r^{(1)}, J_z^{(1)}$ induced by the non-disturbed electric potential component $\Phi^{(1)}(z)$ are:

$$\left.\begin{aligned} J_r^{(1)} &= -\kappa\frac{d}{dr}\Phi^{(1)}(z)=0 \\ J_z^{(1)} &= -\kappa\frac{d}{dz}\Phi^{(1)}(z)=-\frac{\kappa}{h}\Phi_0=-J_0 \end{aligned}\right\} \tag{3}$$

The governing equations and the boundary conditions for the disturbed components $\Phi_i^{(2)}(r,z)$ $(i=1,2)$ are given by:

$$\frac{\partial^2}{\partial r^2}\Phi_i^{(2)}(r,z)+\frac{1}{r}\frac{\partial}{\partial r}\Phi_i^{(2)}(r,z)+\frac{\partial^2}{\partial z^2}\Phi_i^{(2)}(r,z)=0 \quad (i=1,2) \tag{4}$$

$$\left.\begin{aligned} &\frac{\partial}{\partial z}\Phi_1^{(2)}(r,0^+)=-\frac{J_0}{\kappa} \quad (a<r<b) \\ &\Phi_1^{(2)}(r,0^+)=\Phi_2^{(2)}(r,0^-) \quad (0\le r\le a, b\le r<\infty) \end{aligned}\right\} \tag{5}$$

$$\left.\begin{aligned} &\frac{\partial}{\partial z}\Phi_1^{(2)}(r,0^+)=\frac{\partial}{\partial z}\Phi_2^{(2)}(r,0^-) \\ &\frac{\partial}{\partial z}\Phi_1^{(2)}(r,h_1)=0 \\ &\frac{\partial}{\partial z}\Phi_2^{(2)}(r,-h_2)=0 \end{aligned}\right\} \quad (0\le r<\infty) \tag{6}$$

Applying the Hankel integral transform method, the general solutions of the equations (4) can be obtained as follows:

$$\Phi_i^{(2)}(r,z)=\int_0^\infty \left\{\begin{matrix} A_{i1}(s)\exp(-s|z|) \\ +A_{i2}(s)\exp(s|z|) \end{matrix}\right\} J_0(sr)ds \quad (i=1,2) \tag{7}$$

where $J_n(\,)$ is the Bessel function of the first kind of order n, and $A_{ij}(s)\,(i,j=1,2)$ are the unknown functions to be solved. We define the following new unknown function $G_E(r)$ [3]:

$$G_E(r)=\left\{\begin{matrix} \dfrac{\partial}{\partial r}\left[\Phi_1^{(2)}(r,0^+)-\Phi_2^{(2)}(r,0^-)\right] (a<r<b) \\ 0 \qquad\qquad (0\le r\le a, b\le r<\infty) \end{matrix}\right\} \tag{8}$$

Using the boundary conditions (6), the relationships between $A_{ij}(s)\,(i,j=1,2)$ and $G_E(\xi)$ can be obtained as follows:

$$\left.\begin{aligned} A_{11}(s) &= -\frac{1-\exp(-2sh_2)}{2s\{1-\exp(-2sh)\}}L_E(s) \\ A_{12}(s) &= \frac{\exp(-2sh_1)-\exp(-2sh)}{2s\{1-\exp(-2sh)\}}L_E(s) \\ A_{21}(s) &= -\frac{\exp(-2sh_2)-\exp(-2sh)}{2s\{1-\exp(-2sh)\}}L_E(s) \\ A_{22}(s) &= \frac{1-\exp(-2sh_1)}{2s\{1-\exp(-2sh)\}}L_E(s) \end{aligned}\right\} \tag{9}$$

where:

$$L_E(s)=\int_a^b \xi G_E(\xi)J_1(s\xi)d\xi \tag{10}$$

Making use of the first boundary condition (5) with the equations (9), we have the following

singular integral equation for the determination of the unknown function $G_E(\xi)$:

$$\int_a^b \left[M_0(\xi,r) + M_E(\xi,r) \right] \xi G_E(\xi) d\xi = -\frac{2}{\kappa} J_0 \quad (a < r < b) \quad (11)$$

where the integral kernels $M_0(\xi,r)$ and $M_E(\xi,r)$ are given by:

$$M_0(\xi,r) = \begin{cases} \dfrac{2}{\pi} \dfrac{1}{\xi^2 - r^2} E\left(\dfrac{r}{\xi}\right) & (r < \xi) \\ \dfrac{2}{\pi} \left\{ \dfrac{r}{\xi\left(\xi^2 - r^2\right)} E\left(\dfrac{\xi}{r}\right) + \dfrac{1}{r\xi} K\left(\dfrac{\xi}{r}\right) \right\} & (r > \xi) \end{cases} \quad (12)$$

$$M_E(\xi,r) = \int_0^\infty \frac{s J_0(sr) J_1(s\xi)}{1 - \exp(-2sh)} \begin{Bmatrix} 2\exp(-2sh) \\ -\exp(-2sh_1) \\ -\exp(-2sh_2) \end{Bmatrix} ds \quad (13)$$

In the equation (12), $K(\,)$ and $E(\,)$ are complete elliptic integrals of the first and second kinds. For the case of the annular crack $(0 < a < b)$, the singular integral equation (11) is to be solved with the following subsidiary condition obtained from the second boundary condition (5):

$$\int_a^b G_E(\xi) d\xi = 0 \quad (14)$$

To solve the singular integral equation (11) and the additional equation (14) for the annular crack $(0 < a < b)$ and for the penny-shaped crack $(0 = a < b)$, we use the Gauss-Chebyshev or Gauss-Jacobi integration formula [4], respectively. Thus, we can get the solution $G_E(\xi)$.

For the case of $|z| > 0$, substituting the equations (9) with the solution $G_E(\xi)$ to the equations (7), the disturbed components $\Phi_i^{(2)}(r,z)$ $(i = 1,2)$ can be obtained as follows:

$$\Phi_i^{(2)}(r,z) = \frac{(-1)^i}{2} \int_0^\infty \exp\left(-s|z|\right) J_0(sr) L_E(s) ds + \frac{1}{2} \int_0^\infty \frac{J_0(sr) L_E(s)}{1 - \exp(-2sh)} \begin{bmatrix} \exp\{-s(2h - z)\} \\ -\exp\{-s(2h + z)\} \\ +\exp\{-s(2h_1 - z)\} \\ -\exp\{-s(2h_2 + z)\} \end{bmatrix} ds \quad (i = 1,2) \quad (15)$$

For the case of $z \to 0^{\pm}$, the equations (15) will be:

$$\Phi_i^{(2)}(r,0^{\pm}) = \frac{(-1)^i}{2} \int_0^\infty J_0(sr) J_1(s\xi) ds \int_a^b \xi G_E(\xi) d\xi + \frac{1}{2} \int_0^\infty \frac{J_0(sr) L_E(s)}{1 - \exp(-2sh)} \left[\exp(-2sh_1) - \exp(-2sh_2) \right] ds \quad (i = 1,2) \quad (16)$$

The first term of the equation (16) may be:

$$\frac{(-1)^i}{2} \int_0^\infty J_0(sr) J_1(s\xi) ds \int_a^b \xi G_E(\xi) dt = \begin{Bmatrix} \dfrac{(-1)^i}{2} \displaystyle\int_r^b G_E(\xi) d\xi & (a < r < b) \\ 0 & (0 \le r \le a,\ b \le r < \infty) \end{Bmatrix} \quad (i = 1,2) \quad (17)$$

For the case of $|z| > 0$, the disturbed current density components $J_{ri}^{(2)}(r,z)$, $J_{zi}^{(2)}(r,z)$ $(i = 1,2)$ are given by:

$$J_{ri}^{(2)}(r,z) = -\kappa \frac{\partial}{\partial r} \Phi_i^{(2)}(r,z) = \frac{(-1)^i \kappa}{2} \int_0^\infty s \exp\left(-s|z|\right) J_1(sr) L_E(s) ds + \frac{\kappa}{2} \int_0^\infty \frac{s J_1(sr) L_E(s)}{1 - \exp(-2sh)} \begin{bmatrix} \exp\{-s(2h - z)\} \\ -\exp\{-s(2h + z)\} \\ +\exp\{-s(2h_1 - z)\} \\ -\exp\{-s(2h_2 + z)\} \end{bmatrix} ds \quad (i = 1,2) \quad (18)$$

$$J_{zi}^{(2)}(r,z) = -\kappa \frac{\partial}{\partial z} \Phi_i^{(2)}(r,z) = -\frac{\kappa}{2} \int_0^\infty s \exp\left(-s|z|\right) J_0(sr) L_E(s) ds - \frac{\kappa}{2} \int_0^\infty \frac{s J_0(sr) L_E(s)}{1 - \exp(-2sh)} \begin{bmatrix} \exp\{-s(2h - z)\} \\ +\exp\{-s(2h + z)\} \\ +\exp\{-s(2h_1 - z)\} \\ +\exp\{-s(2h_2 + z)\} \end{bmatrix} ds \quad (i = 1,2) \quad (19)$$

Taking the non-continuity of the equation (17) into consideration, the equations (18) and (19) for $z \to 0^{\pm}$ become:

$$J_{ri}^{(2)}(r,0^{\pm}) = -\frac{(-1)^i \kappa}{2} \begin{Bmatrix} G_E(r) & (a < r < b) \\ 0 & (0 \le r \le a,\ b \le r < \infty) \end{Bmatrix} + \frac{\kappa}{2} \int_0^\infty \frac{s J_1(sr) L_E(s)}{1 - \exp(-2sh)} \left[\exp(-2sh_1) - \exp(-2sh_2) \right] ds \quad (i = 1,2) \quad (20)$$

$$J_{z1}^{(2)}(r,0^{+}) = J_{z2}^{(2)}(r,0^{-})$$

$$= \begin{Bmatrix} J_0 & (a < r < b) \\ -\dfrac{\kappa}{2}\displaystyle\int_a^b \left[M_0(\xi, x) + M_E(\xi, x) \right] \xi G_E(\xi) d\xi & \\ & (0 \le r \le a, b \le r < \infty) \end{Bmatrix} \quad (21)$$

IV. Temperature Fields

The heat generation J_0^2 / κ due to only the non-disturbed current density component $J_z^{(1)} = -J_0$ will be ignored. The Poisson's equations with heat generations due to the Joule heating effect induced by the non-disturbed current density component $J_z^{(1)} = -J_0$ and the disturbed current density components $J_{ri}^{(2)}(r,z)$, $J_{zi}^{(2)}(r,z)$ $(i = 1,2)$ are:

$$\lambda \left\{ \frac{\partial^2}{\partial r^2} T_i(r,z) + \frac{1}{r}\frac{\partial}{\partial r} T_i(r,z) + \frac{\partial^2}{\partial z^2} T_i(r,z) \right\} + Q_i(r,z) = 0 \quad (i = 1,2) \quad (22)$$

where:

$$Q_i(r,z) = \frac{1}{\kappa}\left[\left\{ J_{ri}^{(2)}(r,z) \right\}^2 + \left\{ J_{zi}^{(2)}(r,z) - J_0 \right\}^2 - J_0^2 \right] \quad (i = 1,2) \quad (23)$$

The boundary conditions are:

$$\left.\begin{aligned} &\frac{\partial}{\partial z} T_1(r,0^+) = 0 \qquad (a < r < b) \\ &T_1(r,0^+) = T_2(r,0^-) \quad (0 \le r \le a, b \le r < \infty) \end{aligned}\right\} \quad (24)$$

$$\left.\begin{aligned} &\frac{\partial}{\partial z} T_1(r,0^+) = \frac{\partial}{\partial z} T_2(r,0^-) \\ &T_1(r,h_1) = 0 \\ &T_2(r,-h_2) = 0 \end{aligned}\right\} \quad (0 \le r < \infty) \quad (25)$$

Because the Poisson's equations (22) are non-homogeneous, the temperature fields $T_i(r,z)$ $(i = 1,2)$ are given as the sums of the particular integrals $T_i^{(1)}(r,z)$ and the complementary functions $T_i^{(2)}(r,z)$ $(i = 1,2)$:

$$T_i(r,z) = T_i^{(1)}(r,z) + T_i^{(2)}(r,z) \qquad (i = 1,2) \quad (26)$$

The particular integrals $T_i^{(1)}(r,z)$ $(i = 1,2)$ can be obtained by after repeated trial and error as follows:

$$T_i^{(1)}(r,z) = -\frac{1}{\lambda\kappa}\left[\frac{1}{2}\left\{ \Gamma_i(r,z) \right\}^2 + J_0 z \Gamma_i(r,z) \right] \quad (i = 1,2) \quad (27)$$

where $\Gamma_i(r,z)$ $(i = 1,2)$ are:

$$\Gamma_i(r,z) = \frac{(-1)^i \kappa}{2}\int_0^\infty \frac{1}{s} \exp(-s|z|) J_0(sr) L_E(s) ds - \frac{\kappa}{2}\int_0^\infty \frac{J_0(sr) L_E(s)}{s} \begin{bmatrix} F_2(s)\exp\{-s(2h_1 - z)\} \\ -F_1(s)\exp\{-s(2h_2 + z)\} \end{bmatrix} ds \quad (i = 1,2) \quad (28)$$

In the above equations, $F_j(s)$ $(j = 1,2)$ are:

$$F_j(s) = \frac{1 - \exp(-2sh_j)}{1 - \exp(-2sh)} \quad (j = 1,2) \quad (29)$$

For the case of $z \to 0^\pm$, the equations (28) become:

$$\Gamma_i(r,0^\pm) = \begin{Bmatrix} \dfrac{(-1)^i \kappa}{4}\displaystyle\int_r^b G_E(\xi) d\xi \quad (a < r < b) \\ 0 \qquad\qquad (0 \le r \le a, b \le r < \infty) \end{Bmatrix} + \frac{\kappa}{2}\int_0^\infty \frac{J_0(sr) L_E(s)}{1 - \exp(-2sh)} \begin{Bmatrix} \exp(-2sh_1) \\ -\exp(-2sh_2) \end{Bmatrix} ds \quad (i = 1,2) \quad (30)$$

The temperature gradients $q_{zi}^{(1)}(r,z)$ $(i = 1,2)$ in the z -direction are:

$$\begin{aligned} q_{zi}^{(1)}(r,z) &= \frac{\partial}{\partial z} T_i^{(1)}(r,z) \\ &= -\frac{1}{\lambda\kappa}\left[\Gamma_i(r,z)\frac{\partial}{\partial z}\Gamma_i(r,z) + J_0 \Gamma_i(r,z) + J_0 z \frac{\partial}{\partial z}\Gamma_i(r,z) \right] \quad (i = 1,2) \end{aligned} \quad (31)$$

where:

$$\begin{aligned} \frac{\partial}{\partial z}\Gamma_1(r,z) &= \frac{\partial}{\partial z}\Gamma_2(r,z) \\ &= \frac{\kappa}{2}\int_0^\infty s J_0(sr) L_E(s) \exp(-s|z|) ds \\ &\quad - \frac{\kappa}{2}\int_0^\infty s \begin{bmatrix} F_2(s)\exp\{-s(2h_1 - z)\} \\ +F_1(s)\exp\{-s(2h_2 + z)\} \end{bmatrix} J_0(sr) L_E(s) ds \end{aligned} \quad (32)$$

Especially, for the case of $z \to 0^\pm$, the equations (32) become:

$$\frac{\partial}{\partial z}\Gamma_1(r,0^+) = \frac{\partial}{\partial z}\Gamma_2(r,0^-) = \begin{Bmatrix} -J_0 & (a < r < b) \\ \dfrac{\kappa}{2}\displaystyle\int_a^b \left\{ M_0(\xi, r) + M_E(\xi, r) \right\} \xi G_E(\xi) d\xi & \\ & (0 \le r \le a, b \le r < \infty) \end{Bmatrix} \quad (33)$$

Therefore, the temperatures and the temperature gradients shown in the equatins (27) and (31) are:

$$\left.\begin{array}{ll} \dfrac{\partial}{\partial z}T_1^{(1)}(r,0^+)=0 & (a<r<b) \\ T_1^{(1)}(r,0^+)=T_2^{(1)}(r,0^-) & (0\le r\le a, b\le r<\infty) \\ \dfrac{\partial}{\partial z}T_1^{(1)}(r,0^+)=\dfrac{\partial}{\partial z}T_2^{(1)}(r,0^-) & (0\le r<\infty) \end{array}\right\} \tag{34}$$

Because the particular integrals $T_i^{(1)}(r,z)\ (i=1,2)$ do not satisfy the second and third boundary conditions of the equations (25), we have to analyze of the complementary functions $T_i^{(2)}(r,z)\ (i=1,2)$ by the same method used in the electric field analysis.

The governing equations and the boundary conditions for the complementary functions $T_i^{(2)}(r,z)\ (i=1,2)$ are:

$$\frac{\partial^2}{\partial r^2}T_i^{(2)}(r,z)+\frac{1}{r}\frac{\partial}{\partial r}T_i^{(2)}(r,z)+\frac{\partial^2}{\partial z^2}T_i^{(2)}(r,z)=0 \quad (i=1,2) \tag{35}$$

$$\left.\begin{array}{ll} \dfrac{\partial}{\partial z}T_1^{(2)}(r,0^+)=0 & (a<r<b) \\ T_1^{(2)}(r,0^+)=T_2^{(2)}(r,0^-) & (0\le r\le a, b\le r<\infty) \end{array}\right\} \tag{36}$$

$$\left.\begin{array}{l} \dfrac{\partial}{\partial z}T_1^{(2)}(r,0^+)=\dfrac{\partial}{\partial z}T_2^{(2)}(r,0^-) \\ T_1^{(2)}(r,h_1)=-T_1^{(1)}(r,h_1) \\ T_2^{(2)}(r,-h_2)=-T_2^{(1)}(r,-h_2) \end{array}\right\} (0\le r<\infty) \tag{37}$$

The complementary functions $T_i^{(2)}(r,z)\ (i=1,2)$ of the equations (35) can be obtained as follows:

$$T_i^{(2)}(r,z)=\int_0^\infty s\left\{\begin{array}{l} B_{i1}(s)\exp(-s\,|\,z\,|) \\ +B_{i2}(s)\exp(s\,|\,z\,|) \end{array}\right\}J_0(sr)ds \quad (i=1,2) \tag{38}$$

where $B_{ij}(s)\ (i,j=1,2)$ are the unknown functions to be solved. We also define the following new unknown function $G_H(r)$:

$$G_H(r)=\left\{\begin{array}{ll} \dfrac{\partial}{\partial r}\left[T_1^{(2)}(r,0^+)-T_2^{(2)}(r,0^-)\right] & (a<r<b) \\ 0 & (0\le r\le a, b\le r<\infty) \end{array}\right\} \tag{39}$$

Using the boundary conditions (37), the relationships between $B_{ij}(s)\ (i,j=1,2)$ and $G_H(\xi)$ can be obtained as follows:

$$\left.\begin{array}{l} B_{11}(s)=-\dfrac{1+\exp(-2sh_2)}{2\{1-\exp(-2sh)\}}I_H(s) \\ \qquad +\dfrac{\exp(-sh_2)}{1-\exp(-2sh)}\left[\exp(-sh)D_1(s)-D_2(s)\right] \\ B_{12}(s)=\dfrac{\exp(-2sh_1)\{1+\exp(-2sh_2)\}}{2\{1-\exp(-2sh)\}}I_H(s) \\ \qquad -\dfrac{\exp(-sh_1)}{1-\exp(-2sh)}\left[D_1(s)-\exp(-sh)D_2(s)\right] \\ B_{21}(s)=\dfrac{1+\exp(-2sh_1)}{2\{1-\exp(-2sh)\}}I_H(s) \\ \qquad -\dfrac{\exp(-sh_1)}{1-\exp(-2sh)}\left[D_1(s)-\exp(-sh)D_2(s)\right] \\ B_{22}(s)=-\dfrac{\exp(-2sh_2)\{1+\exp(-2sh_1)\}}{2\{1-\exp(-2sh)\}}I_H(s) \\ \qquad +\dfrac{\exp(-sh_2)}{1-\exp(-2sh)}\left[D_1(s)-\exp(-sh)D_2(s)\right] \end{array}\right\} \tag{40}$$

where:

$$I_H(s)=\frac{1}{s}\int_a^b \xi G_H(\xi)J_1(s\xi)d\xi \tag{41}$$

$$\left.\begin{array}{l} D_1(s)=-\dfrac{1}{2}\left[\int_0^\infty \eta f_1(\eta,h_1)J_0(\eta p)d\eta\right]^2 \\ \qquad \times\int_0^\infty pJ_0(sp)dp+h_1f_1(s,h_1) \\ D_2(s)=-\dfrac{1}{2}\left[\int_0^\infty \eta f_2(\eta,-h_2)J_0(\eta p)d\eta\right]^2 \\ \qquad \times\int_0^\infty pJ_0(sp)dp+h_2f_2(s,-h_2) \end{array}\right\} \tag{42}$$

$$\left.\begin{array}{l} f_1(s,h_1)=\dfrac{1}{s}\left[\dfrac{1-\exp(-2sh_2)}{1-\exp(-2sh)}\right]\exp(-sh_1)I_H(s) \\ f_2(s,-h_2)=\dfrac{1}{s}\left[\dfrac{1-\exp(-2sh_1)}{1-\exp(-2sh)}\right]\exp(-sh_2)I_H(s) \end{array}\right\} \tag{43}$$

Making use of the first boundary condition (36) with the equations (40), we have the following singular integral equation for the determination of the unknown function $G_H(\xi)$:

$$\int_a^b\left[M_0(\xi,r)+M_H(\xi,r)\right]\xi G_H(\xi)d\xi = 2\int_0^\infty s\left[N_1(s)D_1(s)-N_2(s)D_2(s)\right]J_0(sr)ds \quad (a<r<b) \tag{44}$$

where the integral kernel $M_H(\xi,r)$ is given by:

$$M_H(\xi,r)=\int_0^\infty \frac{sJ_0(sr)J_1(s\xi)}{1-\exp(-2sh)}\left\{\begin{array}{l} 2\exp(-2sh) \\ +\exp(-2sh_1) \\ +\exp(-2sh_2) \end{array}\right\}ds \tag{45}$$

The known functions $N_j(s)$ $(j=1,2)$ are:

$$\left.\begin{aligned} N_1(s) &= \frac{s\left[\exp(-sh_1)+\exp\{-s(h_2+h)\}\right]}{1-\exp(-2sh)} \\ N_2(s) &= \frac{s\left[\exp(-sh_2)+\exp\{-s(h_1+h)\}\right]}{1-\exp(-2sh)} \end{aligned}\right\} \quad (46)$$

For the case of the annular crack $(0<a<b)$, the singular integral equation (44) is to be solved with the following subsidiary condition obtained from the second boundary condition (36):

$$\int_a^b G_H(\xi)d\xi = 0 \quad (47)$$

We can also solve the singular integral equation (44) and the additional equation (47), and we get the solution $G_H(\xi)$ and the function $I_H(s)$.

Substituting the equations (40) to the equations (38), the complementary functions $T_i^{(2)}(r,z)$ $(i=1,2)$ can be obtained as follows:

$$\begin{aligned} T_i^{(2)}(r,z) &= \frac{1}{2}\int_0^\infty s\begin{bmatrix}(-1)^i\exp(-s|z|)\\ -K_H(s,z)\end{bmatrix} I_H(s)J_0(sr)ds \\ &+\int_0^\infty s\left[K_{D1}(s,z)D_1(s)+K_{D2}(s,z)D_2(s)\right]J_0(sr)ds \end{aligned}$$
$$(i=1,2) \quad (48)$$

where:

$$\left.\begin{aligned} K_H(s,z) &= \frac{1}{1-\exp(-2sh)}\begin{bmatrix}\exp\{-s(2h+z)\}\\ -\exp\{-s(2h-z)\}\\ +\exp\{-s(2h_2+z)\}\\ -\exp\{-s(2h_1-z)\}\end{bmatrix} \\ K_{D1}(s,z) &= \frac{1}{1-\exp(-2sh)}\begin{bmatrix}\exp\{-s(h+h_2+z)\}\\ -\exp\{-s(h_1-z)\}\end{bmatrix} \\ K_{D2}(s,z) &= \frac{1}{1-\exp(-2sh)}\begin{bmatrix}\exp\{-s(h+h_1-z)\}\\ -\exp\{-s(h_2+z)\}\end{bmatrix} \end{aligned}\right\} \quad (49)$$

Furthermore, the temperature gradients are:

$$\begin{aligned} \frac{\partial}{\partial z}T_i^{(2)}(r,z) &= \frac{1}{2}\int_0^\infty s\begin{bmatrix}s\exp(-s|z|)\\ -K'_H(s,z)\end{bmatrix} I_H(s)J_0(sr)ds \\ &+\int_0^\infty s\left[K'_{D1}(s,z)D_1(s)+K'_{D2}(s,z)D_2(s)\right]J_0(sr)ds \end{aligned}$$
$$(i=1,2) \quad (50)$$

where:

$$\left.\begin{aligned} K'_H(s,z) &= \frac{-s}{1-\exp(-2sh)}\begin{bmatrix}\exp\{-s(2h+z)\}\\ +\exp\{-s(2h-z)\}\\ +\exp\{-s(2h_2+z)\}\\ +\exp\{-s(2h_1-z)\}\end{bmatrix} \\ K'_{D1}(s,z) &= \frac{-s}{1-\exp(-2sh)}\begin{bmatrix}\exp\{-s(h+h_2+z)\}\\ +\exp\{-s(h_1-z)\}\end{bmatrix} \\ K'_{D2}(s,z) &= \frac{s}{1-\exp(-2sh)}\begin{bmatrix}\exp\{-s(h+h_1-z)\}\\ +\exp\{-s(h_2+z)\}\end{bmatrix} \end{aligned}\right\} \quad (51)$$

For the case of $z\to 0^{\pm}$, the first terms of the equations (48) and (50) are:

$$\begin{aligned} &\frac{(-1)^i}{2}\int_0^\infty sI_H(s)J_0(sr)ds = \\ &\quad = \begin{cases}\dfrac{(-1)^i}{2}\displaystyle\int_r^b G_H(\xi)d\xi & (a<r<b)\\ 0 & (0\le r\le a,\ b\le r<\infty)\end{cases} \end{aligned}$$
$$(i=1,2) \quad (52)$$

$$\frac{1}{2}\int_0^\infty s^2 I_H(s)J_0(sr)ds = \int_a^b M_0(\xi,r)\xi G_H(\xi)d\xi \quad (53)$$

and consequently:

$$T_1^{(2)}(r,0^+) = T_2^{(2)}(r,0^-) \quad (0\le r\le a,\ b\le r<\infty) \quad (54)$$

$$\begin{aligned} \frac{\partial}{\partial z}T_1^{(2)}(r,0^+) &= \frac{\partial}{\partial z}T_2^{(2)}(r,0^-) \\ &= \frac{1}{2}\int_a^b\left[M_0(\xi,r)+M_H(\xi,r)\right]\xi G_H(\xi)d\xi \\ &\quad -\int_0^\infty s\left[N_1(s)D_1(s)-N_2(s)D_2(s)\right]J_0(sr)ds \end{aligned}$$
$$(0\le r<\infty) \quad (55)$$

Therefore, taking the equation (44) into consideration,

$$\frac{\partial}{\partial z}T_1^{(2)}(r,0^+) = \frac{\partial}{\partial z}T_2^{(2)}(r,0^-) = 0 \quad (a<r<b) \quad (56)$$

For the cases of $z=h_1$ and $z=-h_2$,

$$\left.\begin{aligned} T_1^{(2)}(r,h_1) &= -\int_0^\infty sD_1(s)J_0(sr)ds = -T_1^{(1)}(r,h_1) \\ T_2^{(2)}(r,-h_2) &= -\int_0^\infty sD_2(s)J_0(sr)ds = -T_2^{(1)}(r,-h_2) \end{aligned}\right\} \quad (57)$$

From the equations (54)~(57), the complementary functions $T_i^{(2)}(r,z)$ $(i=1,2)$ satisfy the boundary conditions (36) and (37).

V. Numerical Results and Discussion

To examine the effects of geometric parameters on the electric and temperature fields, the solutions of the singular integral equations have

been obtained and some numerical calculations are carried out. For the numerical calculations, we use the same geometric parameters (h_1, h_2) as ones of the previous paper for the two-dimensional crack [2] to compare the present solutions with the previous results. The results will be presented for the cases of the annular crack and the penny-shaped crack, respectively.

5.1. Annular Crack

In the first series of calculations, we consider the entire trend of the disturbed electric and temperature fields for the case of the annular crack $(0 < a < b)$ and we will also check the validity of the solutions. Figs. 2(a)~(d) show the normalized electric potentials $\Phi_i^{(2)}(r,z)/(J_0 c/\kappa)$, the current densities in the z-direction $J_{zi}^{(2)}(r,z)/J_0$, the temperatures $T_i(r,z)/\left[(J_0 c)^2/\lambda\kappa\right]$ and the temperature gradients $q_{zi}(r,z)/(J_0^2 c/\lambda\kappa)$ $(i=1,2)$ for $h_1/c = 0.5$, $h_2/c = 1.5$ $(h/c = 2.0)$ and $a/c = 2.0$, $b/c = 4.0$. In the figures, z/c shows the normalized position parameter and the solid and dotted lines indicate the fields of $0 \le z \le h_1$ $(i=1)$ and $-h_2 \le z \le 0$ $(i=2)$. It is noted that the disturbed electric and temperature fields satisfy the electric boundary conditions (5), (6) and the temperature boundary conditions (24), (25), respectively, and the obtained solutions should be reasonable.

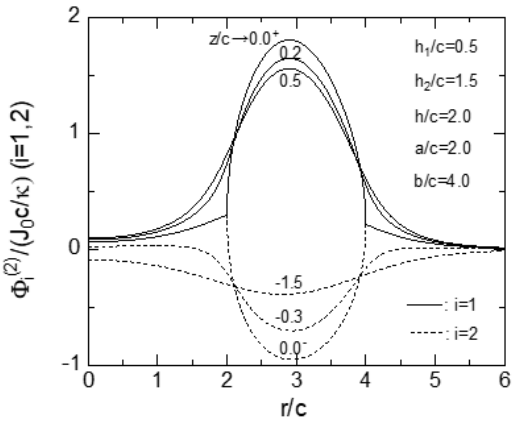

(a)

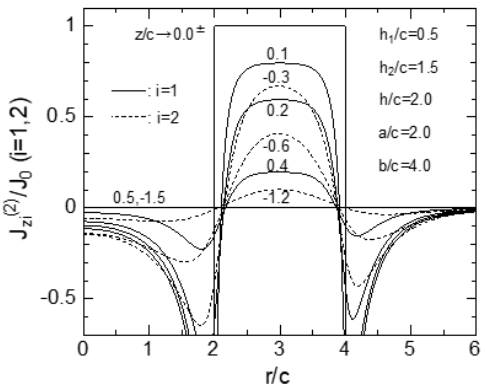

(b)

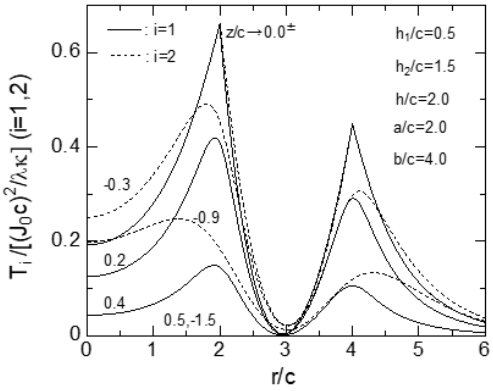

(c)

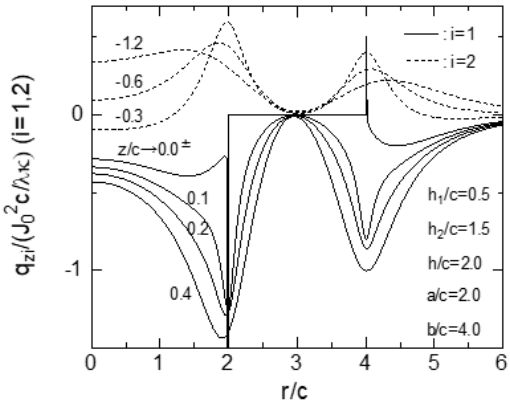

(d)

Fig. 2 The disturbed distributions of the electric potentials (a), the current densities in the z-direction (b), the temperatures (c) and the temperature gradients in the z-direction (d) for $h_1/c = 0.5$, $h_2/c = 1.5$ $(h/c = 2.0)$ and $a/c = 2.0$, $b/c = 4.0$.

The values of $J_{zi}^{(2)}(r,z)$ and $q_{zi}(r,z)$ $(i=1,2)$ have singularity at the crack tip $(r \to a^+, b^-, \quad z \to 0.0^{\pm})$. While the electric and temperature fields are the same as the case of the two-dimensional crack [2], the temperatures $T_1(r,0^+)$ and $T_2(r,0^-)$ on the crack surfaces $(a<r<b)$ are different from each other and the values of $T_1(a,0^+)=T_2(a,0^-)$ are much larger than those of $T_1(b,0^+)=T_2(b,0^-)$. These phenomena cannot be seen for the case of the two-dimensional crack. The temperatures $T_1(r,0^+)$ and $T_2(r,0^-)$ on the outside of the crack $(0 \le r \le a, \; b \le r < \infty)$ decrease with being away from the crack tips $(r=a,b)$. The distribution of the temperatures $T_i(r,z)$ $(i=1,2)$ tend to decrease with increasing $|z|$

In the second set of calculations, we study the influence of the crack position on the temperature distribution. Fig. 3(a) and (b) indicate the normalized temperature along the $z \to 0.0^+$ and 0.0^- planes for the case of $h/c=2.0$ and $a/c=2.0$, $b/c=4.0$. On account of symmetry, we will consider only the case of $0.0 < h_1/c \le 1.0$. Because the temperatures at the upper and lower surfaces of the plate is thermally restricted, the temperatures $T_1(r,0^+)$ and $T_2(r,0^-)$ on the outside of the crack $(0 \le r \le a, b \le r < \infty)$ decrease with decreasing h_1/c. However, the upper and lower surfaces have no serious effect on the temperatures $T_1(x,0^+)$ and $T_2(r,0^-)$ on the crack surfaces $(a<r<b)$. The same tendency can be found in the case of the two-dimensional crack.

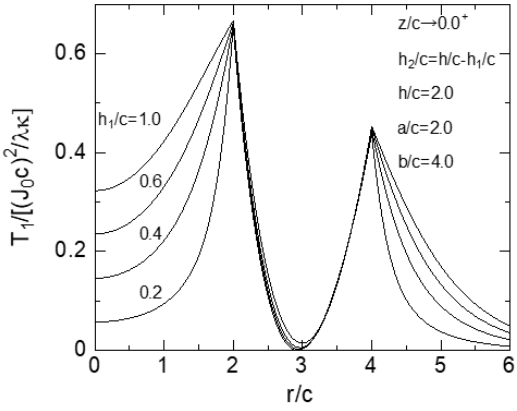

(a)

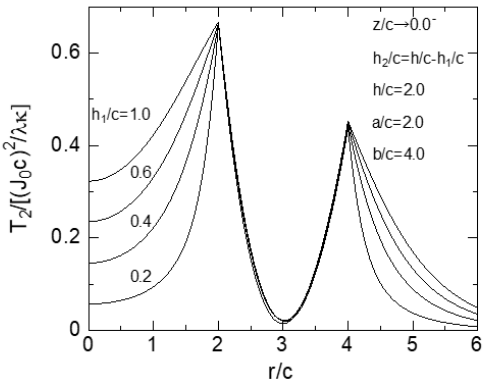

(b)

Fig. 3 The influence of the crack location on the disturbed temperature distribution on the $z/c=0^+$ (a) and 0^- (b) planes for $h/c=2.0$ and $a/c=2.0$, $b/c=4.0$

In the third set of calculations, we study the influence of the crack center location on the disturbed temperature distribution. Figs. 4(a) and (b) show the effect of the crack center location on the normalized temperature distribution $T_i^{(1)}(r,0^{\pm}) / \left[(J_0c)^2/\lambda\kappa\right]$ $(i=1,2)$ along the $z/c \to 0.0^{\pm}$ planes with $h_1/c=0.5$, $h_2/c=1.5$ $(h/c=2.0)$ for various values of $(a+b)/2c$. The dotted line indicates the two-dimensional solution. Of course, the temperatures along $z/c \to 0.0^{\pm}$ on the outside of the crack are $T_1(r,0^+)=T_2(r,0^-)$ $(0 \le r \le a, \; b \le r < \infty)$. As mentioned above, the temperatures along the crack surfaces are $T_1(r,0^+) \ne T_2(r,0^-)$ $(a<r<b)$ and $T_i(a,0^{\pm}) \approx T_i(b,0^{\pm})$ $(i=1,2)$. However, as $(a+b)/2c$ increases, the differences between $T_1(r,0^+)$ and $T_2(r,0^-)$ $(a<r<b)$, $T_i(a,0^{\pm})$ and $T_i(b,0^{\pm})$ $(i=1,2)$ decrease. And for the case of $(a+b)/2c=30.0$, these differences almost disappear and the temperature distributions approach to ones of the two-dimensional case denoted by the dotted line.

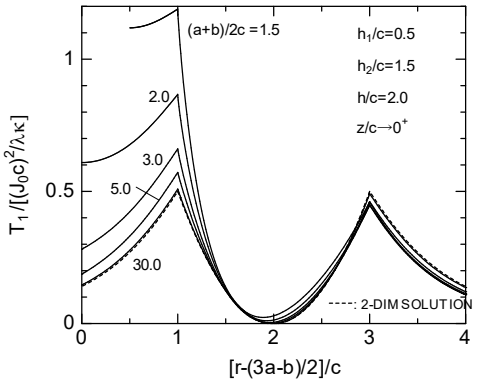

(a)

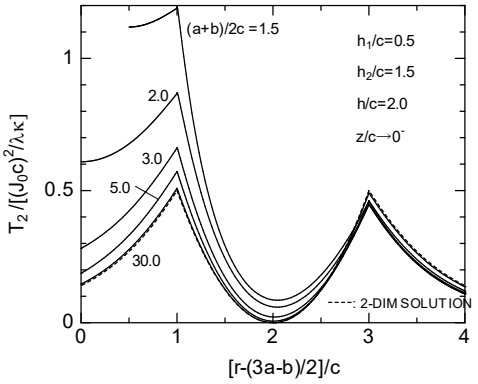

(b)

Fig. 4 The influence of the crack center location on the disturbed temperature distribution along the $z/c \to 0.0^{+}$ (a) and 0.0^{-} (b) planes for $h_1/c = 0.5$, $h_2/c = 1.5$

5-2. Penny-Shaped Crack

In the fourth set of calculations, we also consider the temperature fields for the case of the penny-shaped crack $(0 = a < b)$. Fig. 5 is the same figure as Fig.2(c) indicating the normalized temperature distributions $T_i(r,z) \Big/ \left[(J_0 c)^2/\lambda\kappa\right]$ $(i = 1,2)$ for $h_1/c = 0.5$, $h_2/c = 1.5$ $(h/c = 2.0)$ and $a/c = 0.0$, $b/c = 2.0$. The solid and dotted lines indicate the fields of $0 \le z \le h_1$ $(i = 1)$ and $-h_2 \le z \le 0$ $(i = 2)$. While the entire trend of the temperature distributions is similar to the case of the annular crack, it is noted that the temperatures around the crack center $r/c = 0.0$ become negative for the case of the penny-shaped crack.

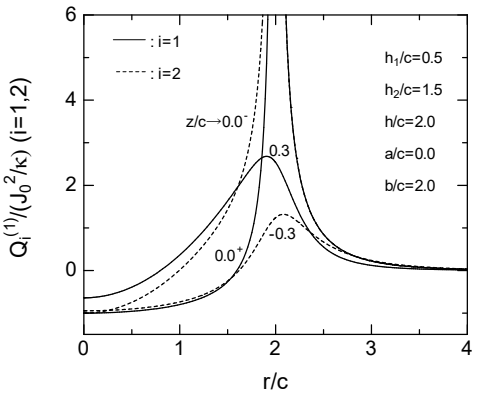

Fig. 5 The temperature distributions for $h_1/c = 0.5$, $h_2/c = 1.5$ $(h/c = 2.0)$ and $a/c = 0.0$, $b/c = 2.0$.

Here, we will check the distributions of the heat generations due to the Joule heating effect defined by the equation (23). Figs. 6(a) and (b) indicate the values of $Q_i(r,z) \Big/ \left[J_0^2/\kappa\right] (i = 1,2)$ for $h_1/c = 0.5$, $h_2/c = 1.5$ $(h/c = 2.0)$, $a/c = 0.0$, $b/c = 2.0$ (a) (Penny-shaped crack) and $a/c = 2.0$, $b/c = 4.0$ (b) (Annular crack). The large positive heat generations occur near the two crack tips $(r = a, b)$ for the case of the annular crack, but the negative heat generation occurs near the center of the penny-shaped crack. This is the reason why the temperatures around the crack center become negative for the case of the penny-shaped crack.

In the final set of calculations, we consider the effect of the crack location on the temperature distribution. Fig. 7 is the same figure as Fig. 3, and denotes the influence of h_1/c on $T_1(r,0^{+})$ and $T_2(r,0^{-})$ for $0.0 < h_1/c \le 1.0$ with $h/c = 2.0$ and $a/c = 0.0$, $b/c = 2.0$. In this case, the upper and lower surfaces have effect on the temperature distributions $T_i(r,0^{\pm})$ $(i = 1,2)$ away from the crack tip $(r = b)$, but the effect becomes small near the crack tip, and the temperatures at the crack tip are $T_1(b,0^{+}) \Big/ \left[(J_0 c)^2/\lambda\kappa\right] = T_2(b,0^{-}) \Big/ \left[(J_0 c)^2/\lambda\kappa\right]$ ≈ 0.5 .

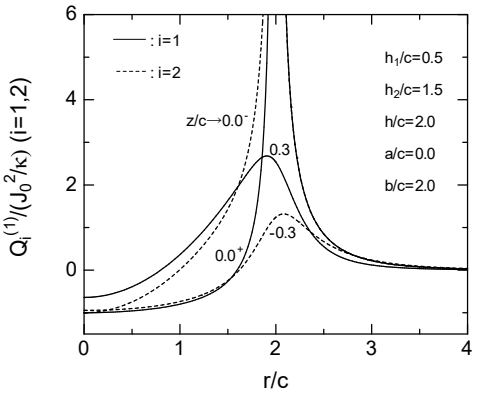

(a)

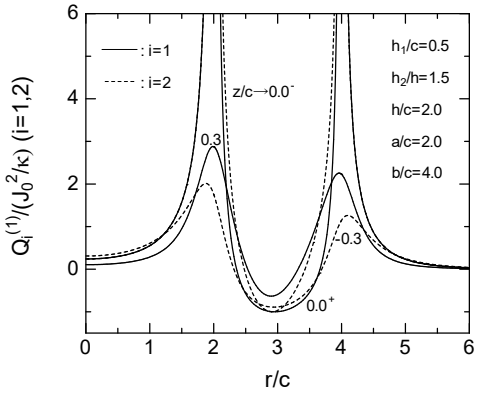

(b)

Fig. 6 The distributions of the heat generation due to the Joule heating effect for $h_1/c=0.5$, $h_2/c=1.5$ $(h/c=2.0)$, $a/c=0.0$, $b/c=2.0$ (a) (Penny-shaped crack) and $a/c=2.0$, $b/c=4.0$ (b) (Annular crack).

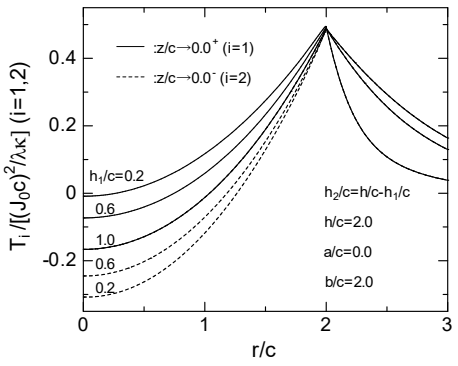

Fig. 7 The influence of the crack location on the disturbed temperature distribution.

VI. Conclusion

The temperature distribution in the plate with the axisymmetric crack during resistance spot welding under a uniform current density is considered in this paper. Using the integral transform method, the electric and temperature fields disturbed by the axisymmetric crack are obtained. The following facts can be found from the numerical results.

6.1. Annular crack

1. The entire trend of the disturbed electric and temperature fields is similar to one for the case of the two-dimensional crack. Namely, the effects of the geometric parameters h_1 and h_2 on the temperature distributions along the crack surfaces are very few, and as the crack approaches to the upper or lower plane, the temperature distributions tend to decrease except for the crack surface temperatures.
2. The temperature distributions depend heavily on the geometric parameters a and b. The crack tip temperatures $T_1(a,0^+) = T_2(a,0^-)$ are larger than the temperatures $T_1(b,0^+) = T_2(b,0^-)$.
3. As the radius of the annular crack $(a+b)/2c$ increases, the temperature distributions are approaching ones for the case of the two-dimensional crack, and the temperature distributions for the case of $(a+b)/2c = 30.0$ agree almost with ones for the case of the two-dimensional crack.

6-2. Penny-shaped crack

1. The geometric parameters h_1 and h_2 have effect on the temperature distributions $T_i(r,0^{\pm})$ $(i=1,2)$ away from the crack tip $(r=b)$, but the effect becomes small near the crack tip.
2. Because of the negative heat generation near the center of the penny-shaped crack, the temperature distributions around the crack center $r/c=0.0$ become negative. This phenomenon cannot be found in the cases of the two-dimensional crack and the annular crack.

References

[1]. T. J-C, Liu, Electro-thermo-structural coupled-field simulation of electric connector with edge crack: *Proceedings of the 6th Asian*

Conference on Mechanics of Functional Materials and Structures (ACMFMS2018), 2018, pp.7-10.

[2]. S. Ueda, R. Imada, D. Kugishima and M.Iyota, Temperature rise associated with a Joule heating effect of a disturbed current density in a plate with a through crack during resistance spot welding, *ISOR Journal of Mechanical and Civil Engineering(ISR-JMCE), 22(5-1)*, 2025, 47-59.

[3]. I. N. Sneddon and M. Lowengrub, *Crack Problems in the Classical Theory of Elasticity* (John Wiley & Sons, Inc., New York, 1969).

[4]. F. Erdogan, G.D. Gupta and T.S. Cook, *Methods of analysis and solution of crack problems* (G. C. Sih (ed), Noordhoff, Leyden, 1972).